Memristive Devices for Quantum Metrology

Memristive devices for quantum metrology

Gianluca Milano[1,2], Federico Ferrarese Lupi[1], Matteo Fretto[1], Carlo Ricciardi[2], Natascia De Leo[1], Luca Boarino[1]*

[1]Advanced Materials Metrology and Life Science Division, INRiM (Istituto Nazionale di Ricerca Metrologica), Strada delle Cacce 91, 10135 Torino, Italy.

[2]Department of Applied Science and Technology, Politecnico di Torino, C.so Duca degli Abruzzi 24, 10129 Torino, Italy.

E-mail: g.milano@inrim.it

Keywords: metrology, quantized conductance, quantum point contact, memristive devices, resistive switching

As a consequence of the redefinition of the International System of Units (SI) where units are defined in terms of fundamental physical constants, memristive devices represent a promising platform for quantum metrology. Coupling ionics with electronics, memristive devices can exhibit conductance levels quantized in multiples of the fundamental quantum of conductance $G_0=2e^2/h$. Since the fundamental quantum of conductance G_0 is related only on physical constants that assume a fixed value in the revised SI, memristive devices can be exploited for the practical realization of a quantum-based resistance standard. Differently from quantum-Hall effect devices conventionally adopted for the realization of a resistance standard whose working principles requires cryogenic temperatures and/or high magnetic fields, memristive devices can operate in air at room temperature without the need of an applied magnetic field. In memristive devices, quantized conductance effects are related to ionic processes at the nanoscale that regulate the resistive switching mechanism underlaying memristive behaviour. Thanks to the high operational speed, high scalability down to the nanometer scale and CMOS compatibility, memristive devices allows on-chip implementation of a resistance standard required for the

,67,7872 1$=,21$/(', 5,&(5&$ 0(752/2*,&
5HSRVLWRU\ ,VWLWX]LRQDOH

0HPULVWLYH 'HYLFHV IRU 4XDQWXP 0HWURORJ\

7KLV LV WKH DXWKRU V VXEPLWWHG YHUVLRQ RI WKH FRQWULEXWLRQ SXE

2ULJLQDO
0HPULVWLYH 'HYLFHV IRU 4XDQWXP 0HWURORJ\ 0LODQR *LDQQXFD)(55$
5LFFLDUGL &DUOR '(/(2 0DULD %RDULQR /XFD ,Q $'9$1&(' 48$1780 7(
S > TXWH @

$YDLODELOLW\
7KLV YHUVLRQ LV DYDLODEOH DW VLQFH 7 =

3XEOLVKHU
:,/(<

3XEOLVKHG
'2, TXWH

7HUPV RI XVH

7KLV DUWLFOH LV PDGH DYDLODEOH XQGHU WHUPV DQG FRQGLWLRQV DV V
GHVFULSWLRQ LQ WKH UHSRVLWRU\

3XEOLVKHU FRS\ULJKW
:,/(<
7KLV DUWLFOH PD\ EH XVHG IRU QRQ FRPPHUFLDO SXUSRVHV LQ DFFRUGD
8VH RI 6HOI $UFKLYHG 9HUVLRQV

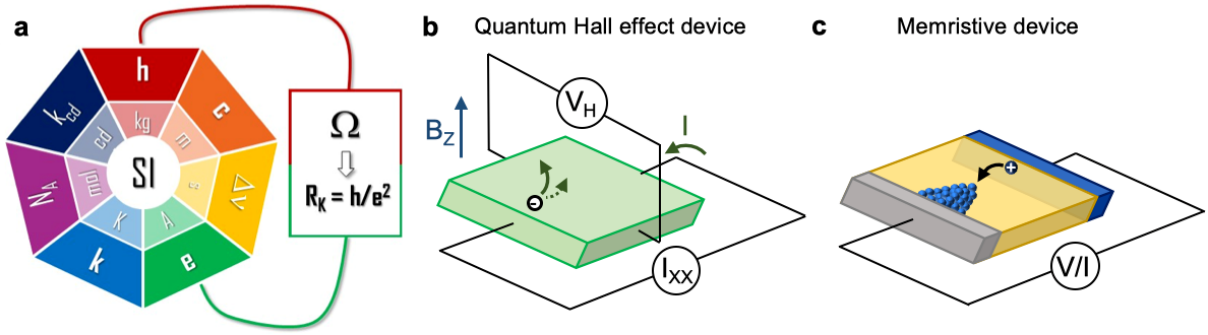

Figure 1. The new SI and the standard of resistance. **a** Units and defining constants in the new SI. The standard of resistance is defined by fixing the values of the fundamental charge *e* and the Planck constant *h*, through the von Klitzing constant R_K. Device configuration for **b** quantum Hall effect involving multiterminal measurements and **c** two-terminal memristive device for observing quantized conductance effects required for the realization of a standard of resistance.

Memristive devices relying on redox-based resistive switching phenomena are two terminal devices where the internal state of resistance depends on the history of applied voltage/current. [10–12] The change of the internal state of resistance under external electrical stimulation of the device, that usually consists of a simple metal/insulator/metal sandwich structure, is related to atomic reconfiguration phenomena involving nanoionic processes.[11] In case of electrochemical metallization memory (ECM) cells, an applied voltage to an electrochemically active electrode (usually Ag or Cu) is responsible for redox reactions involving dissolution of metal atoms to form metal ions that migrate in the insulating matrix under the action of the applied electric field.[13] Subsequent reduction and electro-crystallization of ions leads to the formation of a metallic conductive path (filament) bridging the two electrodes that is responsible for an increased device conductivity. A schematization of the resistive switching mechanism is reported in Fig. 2a. The formation/rupture of this metallic filament under external electrical stimuli leads to the resistive switching behaviour responsible for the change of resistance in between a low resistance state (LRS) and a high resistance state (HRS). Similarly, resistive switching behaviour can be observed in valence change memory (VCM) cells, where ionic species involved in the formation/rupture of the conductive path are oxygen-related

defects such as oxygen vacancies.[11] In both ECM and VCM configuration an initial step termed electroforming process is usually required to initialize the conductive path before observing SET/RESET processes.[14] It is worth noticing that the above described resistive switching phenomena are observed in a wide range of materials such as metal-oxide thin films and nanostructures, perovskites and organic materials.[15–17]

Interestingly, if the size of the conductive filament is reduced to the atomic scale, memristive devices exhibits quantized effects of conductivity typical of ballistic electron transport through a constriction (quantum point contact).[18,19] In such systems, quantum size effects are expected to become relevant when the filament size is in the order of the phase coherence length of the electrons. In this case, the atomic-sized conductive path behaves as an electron waveguide where conduction does not follow the Ohm's law.[20,21] While metal electrodes act as electron reservoirs, the conductive filament bridging the two electrodes results in a ballistic electron conduction path constituted by discrete conductive channels. Each of these conduction channels contributes with a maximum amount of one fundamental quantum of conductance $G_0=2e^2/h$ to the total conductance. Based on the Landauer approach, a quantum point contact (QPC) model describing such quantization of conductance in memristive devices was proposed by Miranda et al..[22] In the QPC model, quantum transport through a 3D tube-like constriction can be described by means of a 1D tunneling behavior. In this case, the energy dispersion curve of electrons consists of discrete parabolic sub-bands, where the spacing in between sub-bands depends on the filament morphology. In this framework, the electronic current flowing through the quantum point contact under application of an external bias V is given by the expression:[18,19]

$$I(V) = \frac{2e}{h} N \int_{-\infty}^{\infty} T(E)[f(E - \beta eV) - f(E + (1 - \beta)eV]dE \quad (1)$$

where N (integer number), is the number of the 1D conductive channels contributing to the conduction, T is the transmission probability, E is the energy, f is the Fermi distribution, e the

electron charge, h is the Planck constant and β is the asymmetry parameter representing the fraction of the applied bias that drops on the source side of the constriction ($0 \leq \beta \leq 1$). Considering the expression for T derived from the assumption of an inverted parabolic potential barrier for the quantized sub-bands into the constriction:[18,19,23]

$$T(E) = \{1 + exp[-\alpha(E - \varphi)]\}^{-1} \quad (2)$$

where α is a constant related to the potential barrier curvature of the sub-bands and φ is the barrier height, by inserting eq. (2) in eq. (1), the expression for I can be rewritten as:[18,19,23]

$$I(V) = \frac{2e}{h} N \left\{ eV + \frac{1}{\alpha} ln \left[\frac{1+exp\{\alpha[\varphi-\beta eV]\}}{1+exp\{\alpha[\varphi+(1-\beta)eV]\}} \right] \right\} \quad (3)$$

Note that eq. (3) can describe both HRS and LRS of a memristive device by properly adjusting the values of α and φ. In the HRS, where conductive filament is not continuous, for low applied voltages eq. (3) converges to:[18]

$$I(V) = NG_0 exp\,(-\alpha\varphi)\,V \quad (4)$$

In this case, the electronic conduction is regulated by the barrier that is described by α and φ parameters. In the LRS, where the metallic conductive filament is continuous, eq. (3) converges to:[18]

$$I(V) = N\beta G_0 V \quad (5)$$

Thus, the conductance shows integer multiples of the fundamental quantum of conductance G_0 when the voltage drop across the two interfaces is asymmetric (β=1), according to the relationship:

$$G = NG_0 \quad (6)$$

In this case, it turns out that the quantized conductance values depend only on constant of Nature fixed to an exact value in the new SI and are related to the von Klitzing constant through the relation $G_0=2/R_K$. Since the Fermi wavelength in a metal is of the same order of magnitude of atomic separation,[20] a quantum point contact in memristive devices requires atomic dimensions of the filament where the number of activated conductive channels (N) depends on

its size and geometry. As schematized in figure 2b, the memristive cell exhibit $G<<G_0$ when the device is in the HRS and electronic conduction can occur through tunneling effects across the filament gap, $G\sim G_0$ when the filament size is close to the atomic scale while $G>>G_0$ by increasing the filament size to few nanometers where conduction occurs according to the Ohm's law and quantum effects are suppressed. An important aspect is that quantum conductance effects can be observed at room temperature since the quantum mode splitting is typically in the order of about 1 eV.[21]

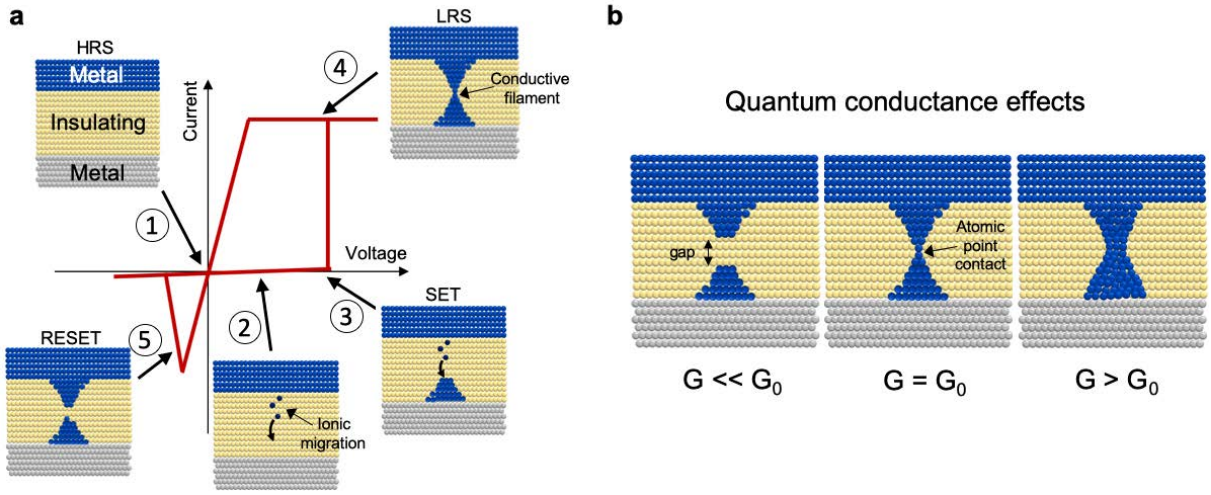

Figure 2. Resistive switching phenomena and quantum conductance effects in memristive devices. **a** Working principle of a memristive device involving nanoionics processes with formation/rupture of a conductive path (filament) across the insulating layer that is responsible for resistive switching behaviour from an high resistance state (HRS) to a low resistance state (LRS) and viceversa. **b** Quantum conductance effects can be observed when the filament is scaled down to the atomic scale. Electronic conduction occurs through tunneling with $G<<G_0$ when the filament is not continuous (HRS state), filament with atomic size results in $G\sim G_0$ while $G>>G_0$ when the filament size is increased to few nanometers.

Despite the observation of quantized conductance values in resistive switching devices already in the '90s,[24,25] the interest on memristive devices exhibiting quantized conductance becomes relevant after that Terabe et al.[26] reported in 2005 high control of quantized conductance values in two-terminal atomic switch memristive devices. In this work, well defined quantized conductance levels were obtained by electrochemically controlling the growth/rupture of a silver protusion in a silver-sulphide (Ag_2S) matrix through external electrical stimulation. After

this seminal work, experimental evidences of conductance quantization were reported in a wide range of memristive cells based on different material systems both in ECM and VCM configuration.[27,28,37–39,29–36] Independently from the memristive mechanism, the observation of quantum effects requires an accurate control of the filament size and morphology at the atomic level by means of appropriate external electrical stimulations of the device. In this context, quantized conductance effects have been reported by means of a wide range of operating methods employed to probe the memristive device response to external electrical stimulations. The most common method of stimulation is the voltage sweep mode where a voltage ramp is applied to the device. Under this stimulation, quantized steps of conductance were reported during both SET and RESET operations as a consequence of the progressive formation and rupture of the filament, respectively[18,27,42,30,31,33,35,37,39–41] An example of quantization phenomena observed during the RESET process in Pt/HfO_2/Pt memristive devices by Li et al.[18] is reported in Fig. 3a. As can be observed, a voltage sweep applied to the device resulted in a gradual RESET process with an increasing of device resistance in a quantized manner due to the progressive rearrangement of atoms during the final stage of filament dissolution. During voltage sweeps, the filament morphology responsible for quantized resistance levels can be also modulated by controlling the maximum current flowing into the device and/or by the applied voltage range.[35] Current sweep operation mode was reported by Tappertzhofen et al.[36] to be responsible for the observation of more discrete resistance levels compared to the voltage sweep operation mode in AgI memristive cells. Quantized steps of conductance can be observed also in constant voltage bias operation mode.[27,28,34,40] Indeed, when an appropriate bias voltage is applied to the cell, a stepwise increasing/decreasing of conductivity with multiples of G_0 can be observed over a large time scale. For example, this effect was reported by Tsuruoka et al.[28] in Ag/Ta_2O_5/Pt memristive cells where quantized conductance steps are observed in the current time trace under the application of a small constant bias. As an alternative, the internal resistance state can be changed at steps of quantum conductance under device stimulation by

means of voltage pulses.[28–30,41] By properly adjusting pulse parameters such as amplitude, width and time interval between pulses, quantized conductance levels can be observed in both SET and RESET processes as reported in Figure 3d and e. It is worth noticing that the modulation of the quantized conductance levels was demonstrated by device stimulation with pulses down to the nanosecond timescale,[29] making memristive devices particularly promising for the realization of high-speed metrological devices.

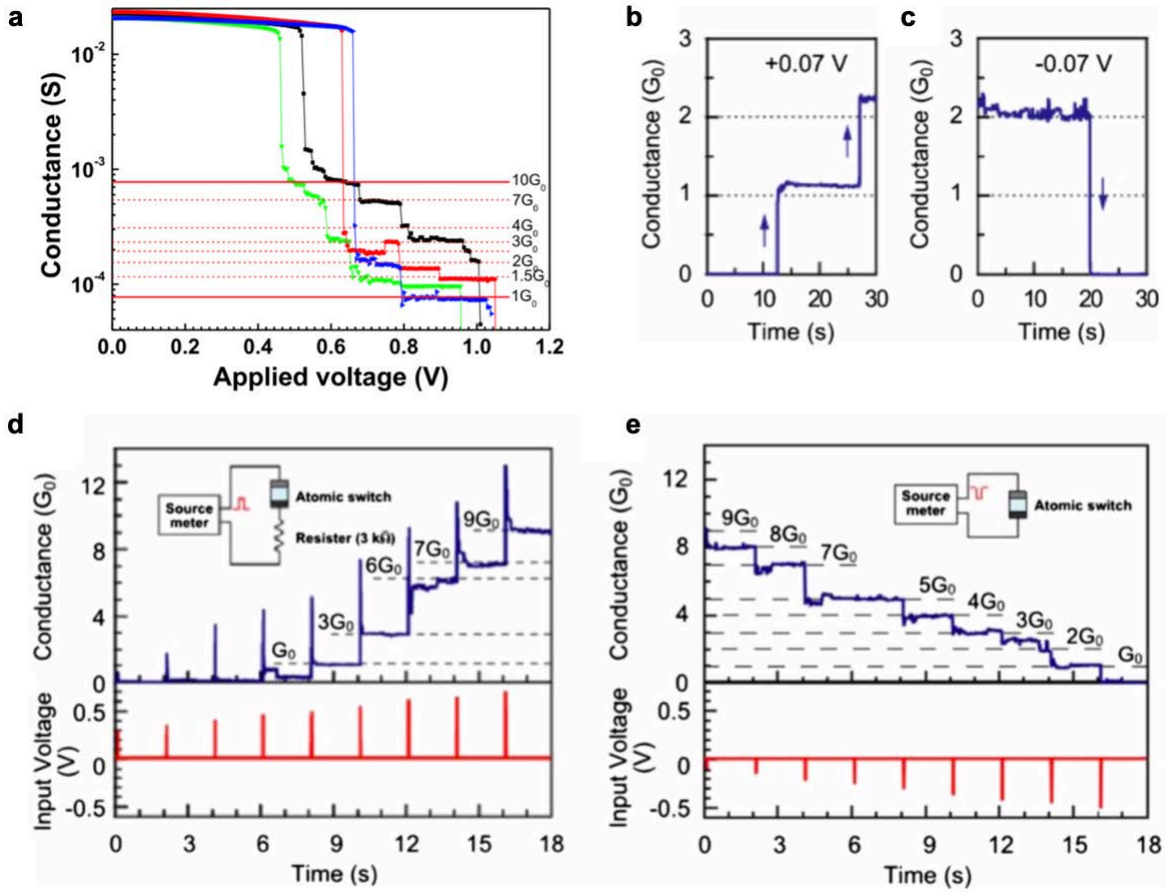

Figure 3. Quantum conductance effects in memristive devices. **a** Quantization phenomena observed in Pt/HfO_2/Pt memristive devices during the RESET process in voltage sweep operation mode. Reproduced under the terms of Creative Commons Attribution 4.0 License.[18] Copyright 2015, Springer. Stepwise change of conductance in Ag/Ta2O5/Pt memristive devices in constant voltage bias operation mode during **b** SET and **c** RESET processes; modulation of the internal state of the memristive device in voltage pulse operational mode during **d** SET and **e** RESET process. During SET (panel d), a resistor was inserted in series to the memristive device in order to limit the maximum allowed current. Reproduced with permission.[28] Copyright 2012, IOP Publishing.

induced quantum point contacts realized by manipulating ions with consequent atomic rearrangement at the nanoscale. This means that ionic processes are coupled to the electronic ones, differently from conventional quantum-Hall devices where quantized conductance levels are determined only by purely electronic phenomena occurring in presence of an external magnetic field. As a direct consequence of coupling ionics with electronics in two-terminal memristive devices, it is possible to observe quantized conductance phenomena in air at room temperature and without applying any external magnetic field. In perspective, particularly promising results the scalability of the memristive device that was demonstrated down to the critical size of < 2 nm[47] , the high operational speed (< 1ns)[48] and the low power consumption for programming the internal conductance state (<pJ)[49]. In addition, it is worth noticing that common materials for memristive devices such as transition metal oxides, perovskites and metal electrodes are compatible with CMOS technology not only in terms of materials and processing techniques but also in terms of electrical performances.[50,51] All these characteristics makes memristive devices particularly promising for on-chip integration of a standard of resistance. In the light of the new SI, this represents an important breakthrough for electrical metrology, allowing the realization of embedded self-calibrating systems and equipments with traceability to the fundamental physical quantities. Also, it is important to mention that a standard of resistance coupled with a voltage standard (realized for example by exploiting the Josephson effect) is a possible route for the practical realization of a current standard as indicated by the Bureau International des Poids et Mesures.[4] However, the main challenges for exploiting memristive devices for metrology are related to the intrinsic stochasticity of ionic processes underlaying resistive switching effects that affect reproducibility and variability over time of quantized conductance levels. In order to overcome these issues, a deep understanding and control nanoionics processes underlaying memristive behaviour is required. Moreover, one of the main challenges still remain to uncover the relationship between the involved materials and device functionalities. In this scenario, the development of memristive devices with

quantized conductance levels for the realization of a resistance standard necessarily imply an optimization of the involved materials and their interfaces as well as the operating conditions. All these challenges towards the realization of a resistance standard based on memristive devices have to be faced by taking into consideration the level of uncertainty required for each specific application.

Received: ((will be filled in by the editorial staff))
Revised: ((will be filled in by the editorial staff))
Published online: ((will be filled in by the editorial staff))

References

[1] J. Fischer, J. Ullrich, *Nat. Phys.* **2016**, *12*, 4.
[2] E. Göbel, U. Siegner, *The New International System of Units (SI)*, Wiley, **2019**.
[3] F. Piquemal, B. Jeckelmann, L. Callegaro, J. Hällström, T. J. B. M. Janssen, J. Melcher, G. Rietveld, U. Siegner, P. Wright, M. Zeier, *Metrologia* **2017**, *54*, R1.
[4] BIPM Bureau International des Poids et Mesures, *The International System of Units (SI Brochure) [9th Edition]*, **2019**.
[5] W. Poirier, S. Djordjevic, F. Schopfer, O. Thévenot, *Comptes Rendus Phys.* **2019**, *20*, 92.
[6] K. von Klitzing, *Nat. Phys.* **2017**, *13*, 198.
[7] K. V. Klitzing, G. Dorda, M. Pepper, *Phys. Rev. Lett.* **1980**, *45*, 494.
[8] K. von Klitzing, *Rev. Mod. Phys.* **1986**, *58*, 519.
[9] K. S. Novoselov, Z. Jiang, Y. Zhang, S. V. Morozov, H. L. Stormer, U. Zeitler, J. C. Maan, G. S. Boebinger, P. Kim, A. K. Geim, *Science (80-.).* **2007**, *315*, 1379.
[10] D. B. Strukov, G. S. Snider, D. R. Stewart, R. S. Williams, *Nature* **2008**, *453*, 80.
[11] R. Waser, R. Dittmann, G. Staikov, K. Szot, *Adv. Mater.* **2009**, *21*, 2632.
[12] R. Waser, M. Aono, *Nat. Mater.* **2007**, *6*, 833.
[13] I. Valov, R. Waser, J. R. Jameson, M. N. Kozicki, *Nanotechnology* **2011**, *22*, 289502.
[14] J. Joshua Yang, F. Miao, M. D. Pickett, D. A. A. Ohlberg, D. R. Stewart, C. N. Lau, R. S. Williams, *Nanotechnology* **2009**, *20*, 215201.
[15] A. Sawa, *Mater. Today* **2008**, *11*, 28.
[16] G. Milano, S. Porro, I. Valov, C. Ricciardi, *Adv. Electron. Mater.* **2019**, *5*, 1800909.
[17] W.-P. Lin, S.-J. Liu, T. Gong, Q. Zhao, W. Huang, *Adv. Mater.* **2014**, *26*, 570.
[18] Y. Li, S. Long, Y. Liu, C. Hu, J. Teng, Q. Liu, H. Lv, J. Suñé, M. Liu, *Nanoscale Res. Lett.* **2015**, *10*, 420.
[19] W. Xue, S. Gao, J. Shang, X. Yi, G. Liu, R. Li, *Adv. Electron. Mater.* **2019**, *5*, 1800854.
[20] H. van Houten, C. Beenakker, *Phys. Today* **1996**, *49*, 22.
[21] N. Agraït, *Phys. Rep.* **2003**, *377*, 81.
[22] E. Miranda, D. Jimenez, J. Sune, *IEEE Electron Device Lett.* **2012**, *33*, 1474.
[23] X. Lian, X. Cartoixà, E. Miranda, L. Perniola, R. Rurali, S. Long, M. Liu, J. Suñé, *J. Appl. Phys.* **2014**, *115*, 244507.
[24] J. Hajto, A. E. Owen, S. M. Gage, A. J. Snell, P. G. LeComber, M. J. Rose, *Phys. Rev. Lett.* **1991**, *66*, 1918.
[25] E. Yun, M. F. Becker, R. M. Walser, *Appl. Phys. Lett.* **1993**, *63*, 2493.

[26] K. Terabe, T. Hasegawa, T. Nakayama, M. Aono, *Nature* **2005**, *433*, 47.
[27] J. Zhao, Z. Zhou, Y. Zhang, J. Wang, L. Zhang, X. Li, M. Zhao, H. Wang, Y. Pei, Q. Zhao, Z. Xiao, K. Wang, C. Qin, G. Wang, H. Li, B. Ding, F. Yan, K. Wang, D. Ren, B. Liu, X. Yan, *J. Mater. Chem. C* **2019**, *7*, 1298.
[28] T. Tsuruoka, T. Hasegawa, K. Terabe, M. Aono, *Nanotechnology* **2012**, *23*, 435705.
[29] L. Jiang, L. Xu, J. W. Chen, P. Yan, K. H. Xue, H. J. Sun, X. S. Miao, *Appl. Phys. Lett.* **2016**, *109*, 153506.
[30] C. Chen, S. Gao, F. Zeng, G. Y. Wang, S. Z. Li, C. Song, F. Pan, *Appl. Phys. Lett.* **2013**, *103*, 043510.
[31] F. G. Aga, J. Woo, J. Song, J. Park, S. Lim, C. Sung, H. Hwang, *Nanotechnology* **2017**, *28*, 115707.
[32] C. Hu, M. D. McDaniel, A. Posadas, A. A. Demkov, J. G. Ekerdt, E. T. Yu, *Nano Lett.* **2014**, *14*, 4360.
[33] E. Miranda, S. Kano, C. Dou, K. Kakushima, J. Suñé, H. Iwai, *Appl. Phys. Lett.* **2012**, *101*, 012910.
[34] X. Zhao, H. Xu, Z. Wang, L. Zhang, J. Ma, Y. Liu, *Carbon N. Y.* **2015**, *91*, 38.
[35] X. Zhu, W. Su, Y. Liu, B. Hu, L. Pan, W. Lu, J. Zhang, R.-W. Li, *Adv. Mater.* **2012**, *24*, 3941.
[36] S. Tappertzhofen, I. Valov, R. Waser, *Nanotechnology* **2012**, *23*, 145703.
[37] A. Mehonic, A. Vrajitoarea, S. Cueff, S. Hudziak, H. Howe, C. Labbé, R. Rizk, M. Pepper, A. J. Kenyon, *Sci. Rep.* **2013**, *3*, 2708.
[38] W. Banerjee, H. Hwang, *Adv. Electron. Mater.* **2019**, *1900744*, 1900744.
[39] S. U. Sharath, S. Vogel, L. Molina-Luna, E. Hildebrandt, C. Wenger, J. Kurian, M. Duerrschnabel, T. Niermann, G. Niu, P. Calka, M. Lehmann, H.-J. Kleebe, T. Schroeder, L. Alff, *Adv. Funct. Mater.* **2017**, *27*, 1700432.
[40] S. Long, X. Lian, C. Cagli, X. Cartoixà, R. Rurali, E. Miranda, D. Jiménez, L. Perniola, M. Liu, J. Suñé, *Appl. Phys. Lett.* **2013**, *102*, 183505.
[41] A. Younis, D. Chu, S. Li, *J. Mater. Chem. C* **2014**, *2*, 10291.
[42] K. Krishnan, M. Muruganathan, T. Tsuruoka, H. Mizuta, M. Aono, *Adv. Funct. Mater.* **2017**, *27*, 1605104.
[43] I. Valov, E. Linn, S. Tappertzhofen, S. Schmelzer, J. van den Hurk, F. Lentz, R. Waser, *Nat. Commun.* **2013**, *4*, 1771.
[44] G. Milano, M. Luebben, Z. Ma, R. Dunin-Borkowski, L. Boarino, C. F. Pirri, R. Waser, C. Ricciardi, I. Valov, *Nat. Commun.* **2018**, *9*, 5151.
[45] W. Wang, M. Wang, E. Ambrosi, A. Bricalli, M. Laudato, Z. Sun, X. Chen, D. Ielmini, *Nat. Commun.* **2019**, *10*, 81.
[46] S. Tappertzhofen, E. Linn, S. Menzel, A. J. Kenyon, R. Waser, I. Valov, *IEEE Trans. Nanotechnol.* **2015**, *14*, 505.
[47] S. Pi, C. Li, H. Jiang, W. Xia, H. Xin, J. J. Yang, Q. Xia, *Nat. Nanotechnol.* **2019**, *14*, 35.
[48] B. J. Choi, A. C. Torrezan, J. P. Strachan, P. G. Kotula, A. J. Lohn, M. J. Marinella, Z. Li, R. S. Williams, J. J. Yang, *Adv. Funct. Mater.* **2016**, *26*, 5290.
[49] F. Hui, E. Grustan-Gutierrez, S. Long, Q. Liu, A. K. Ott, A. C. Ferrari, M. Lanza, *Adv. Electron. Mater.* **2017**, *3*, 1600195.
[50] S. H. Jo, W. Lu, *Nano Lett.* **2008**, *8*, 392.
[51] F. Cai, J. M. Correll, S. H. Lee, Y. Lim, V. Bothra, Z. Zhang, M. P. Flynn, W. D. Lu, *Nat. Electron.* **2019**, *2*, 290.

Memristive devices exhibiting quantum conductance levels are proposed as quantum metrology devices in the light of the redefinition of the International System of Units (SI). Due to their high scalability, compatibility with CMOS technology, memristive devices working in air at room temperature represent promising platforms for on-chip embedding of a resistance standard for realizing self-calibrating systems with zero-chain traceability.

Quantum metrology

Gianluca Milano*, Federico Ferrarese Lupi, Matteo Fretto, Carlo Ricciardi, Natascia De Leo, Luca Boarino

Memristive devices for quantum metrology